Development 130, 401-410

doi:10.1242/dev.00215

DEVELOPMENT AND DISEASE

Hypogonadotropic hypogonadism and peripheral neuropathy in *Ebf2*-null mice

Anna Corradi[1,*], Laura Croci[1,2,*], Vania Broccoli[2], Silvia Zecchini[1,2], Stefano Previtali[1], Wolfgang Wurst[3], Stefano Amadio[1], Roberto Maggi[4], Angelo Quattrini[1] and G. Giacomo Consalez[1,2,†]

[1]San Raffaele Scientific Institute, Milan, Italy
[2]Stem Cell Research Institute, San Raffaele Scientific Institute, Milan, Italy
[3]Max Planck Institute of Psychiatry, Munich, and GSF-Research Center of Environment and Health, Institute of Developmental Genetics, Neuherberg, Germany
[4]CEND, Department of Endocrinology, University of Milan, Italy

*These authors contributed equally to this work
†Author for correspondence (e-mail: g.consalez@hsr.it)

Accepted 18 October 2002

SUMMARY

Olf/Ebf transcription factors have been implicated in numerous developmental processes, ranging from B-cell development to neuronal differentiation. We describe mice that carry a targeted deletion within the *Ebf2* (O/E3) gene. In *Ebf2*-null mutants, because of defective migration of gonadotropin releasing hormone-synthesizing neurons, formation of the neuroendocrine axis (which is essential for pubertal development) is impaired, leading to secondary hypogonadism. In addition, *Ebf2*$^{-/-}$ peripheral nerves feature defective axon sorting, hypomyelination, segmental dysmyelination and axonal damage, accompanied by a sharp decrease in motor nerve conduction velocity. *Ebf2*-null mice reveal a novel genetic cause of hypogonadotropic hypogonadism and peripheral neuropathy in the mouse, disclosing an important role for *Ebf2* in neuronal migration and nerve development.

Key words: Olf/Ebf genes, Neurogenesis, Neural development, Neuronal migration, Neuroendocrine, GnRH neurons, Peripheral nerve, Peripheral neuropathy, Dysmyelination, Homologous recombination, Knockout, Targeted inactivation, Gene targeting, COE2, O/E3

INTRODUCTION

Olf/Ebf genes (Garel et al., 1997; Hagman et al., 1993; Malgaretti et al., 1997; Wang and Reed, 1993; Wang et al., 1997) (reviewed by Dubois and Vincent, 2001) (herein referred to as Ebf genes, in agreement with the accepted mouse nomenclature) encode transcription factors strikingly conserved in evolution from pseudocoelomates to chordates. These transcription factors contain an HLH dimerization domain and a characteristic DNA binding domain featuring a C-C-H-H zinc-finger motif. In vitro, these proteins bind an imperfect palindromic DNA consensus sequence, both as homo- and heterodimers. Albeit originally identified for their roles in the immune system (Hagman et al., 1993), Ebf genes have been implicated in various aspects of neural development (Dubois et al., 1998; Garel et al., 1999; Malgaretti et al., 1997; Pozzoli et al., 2001; Prasad et al., 1998) and neuronal function (Kudrycki et al., 1993). Specifically, they have been found to play roles in ventral nerve cord fasciculation in *C. elegans* (Prasad et al., 1998) and axon navigation (Garel et al., 1999), as well as neuronal migration (Garel et al., 2000) and differentiation (Dubois et al., 1998; Pozzoli et al., 2001; Prasad et al., 1998) in various organisms. Several in vivo studies have disclosed genetic interactions between Ebf genes and some of the most important regulators of neural development, including hedgehog (Vervoort et al., 1999) and Notch (Crozatier and Vincent, 1999). All the above data suggest a potential role for Ebf genes in short-range dorsoventral patterning and morphogenesis of the embryonic nervous system.

Three mammalian Ebf genes have been isolated so far: *Ebf1*, *Ebf2* and *Ebf3*. An additional member of the family, *O/E4*, was isolated more recently (Wang et al., 2002) and its expression in the embryonic neural tube has not been mapped to date. In the embryonic mouse nervous system, *Ebf1*, *Ebf2* and *Ebf3* are transcribed in partially overlapping territories (Garel et al., 1997), but display significant differences in their distributions (Garel et al., 1997; Malgaretti et al., 1997), suggesting that each may play roles in the morphogenesis of different head territories. As one example, *Ebf1* is the only family member expressed in the striatal anlage (Garel et al., 1997). Second, noticeable differences are observed in the distribution of Ebf transcripts across the wall of the neural tube (NT): *Ebf1* and *Ebf3*, which map to mouse chromosomes 11 and 7, respectively (Garel et al., 1997), are co-expressed at most sites in the mantle layer of the developing NT, whereas *Ebf2*, which maps to mouse chromosome 14, is expressed by younger postmitotic neural cells located in the subventricular layer of the prospective spinal cord (Garel et al., 1997; Malgaretti et al.,

1997). In the developing nervous system, the functions of *Ebf1* and *Ebf3* appear to be somewhat redundant, in that *Ebf1*$^{-/-}$ mutants feature defects in neuronal differentiation (Garel et al., 1999) and short-range neuronal migration (Garel et al., 2000) only in territories in which *Ebf3* is not expressed. However, no genetic evidence is available regarding the specific role of *Ebf2* in the context of vertebrate neural development. Again, overexpression studies conducted in *Xenopus*, where an *Ebf1* ortholog has not been isolated to date, indicate that *Xebf2/Xcoe2* (Dubois et al., 1998; Pozzoli et al., 2001) is expressed earlier than *Xebf3* (Pozzoli et al., 2001), and suggest that the two genes may play distinct roles in the context of primary neurogenesis (Pozzoli et al., 2001). In particular, gain-of-function experiments suggest that *Xebf2* and *Xebf3* differ in their sensitivity to lateral inhibition (Pozzoli et al., 2001). In fact, *Notch* activation can suppress the ability of *NeuroD* (*Neurod1* – Mouse Genome Informatics) to promote *Xebf2* but not *Xebf3* transcription (Pozzoli et al., 2001). Finally, lateral inhibition interferes with the ability of overexpressed *Xebf2*, but not *Xebf3*, to activate transcription of early (N-tubulin) and late (NF-M) neuronal differentiation markers (Pozzoli et al., 2001). These results indicate that *Notch* activation interferes in a cell-autonomous fashion with *Ebf2* function, not just with its transcription.

The features and interactions common to the entire Ebf gene family in phylogeny, as well as the specific features of the *Ebf2* homolog in *Xenopus* neurogenesis prompted us to study the contribution of *Ebf2* (Malgaretti et al., 1997) to neural development and function, using a genetic approach in the mouse. *Ebf2*$^{-/-}$ mice were generated by gene targeting, and revealed a key role for *Ebf2* in the embryonic migration of gonadotropin-releasing hormone (GnRH)-synthesizing neurons from the vomeronasal organ to the hypothalamus. In addition, our results implicated this gene in peripheral nerve morphogenesis.

MATERIALS AND METHODS

Animal care

All experiments described in this paper were conducted in agreement with the stipulations of the San Raffaele Scientific Institute Animal Care and Use Committee.

Construction of Ebf2 gene targeting vector

Eleven *Ebf2* genomic clones were isolated by screening of a 129/SvJ mouse genomic library (10^6 pfu) with an *Ebf2*-specific intronic probe. the probe was derived by restriction of a PCR product obtained with a forward primer from exon 1 and a reverse primer from exon 3 (F: 5′-CTG GGT GCC GAG ATG GAT T; R: 5′-TGT TGG TCT TCT CAT TGC CTT). We used a modified pPNT vector containing a *Neo* cassette flanked by *LoxP* sites. The construct contains a *PGK-tk* cassette downstream of the 3′ arm of homology. After homologous recombination, 5.5 kb of genomic sequence were deleted from the *Ebf2* gene, including the putative translation initiation site and the first five exons.

Generation of recombinant embryonic stem (ES) cells

ES cells (TBV2 line) were grown in Dulbecco's Modified Eagles Medium (DMEM) (Gibco), 15% fetal calf serum (Gibco), 10^{-4} M β-mercaptoethanol (Gibco), 2 mM L-Glutamine and 1000 U/ml LIF (Heiko), on an embryonic fibroblast feeder layer previously inactivated with Mitomycin C. Electroporation, positive and negative selection were performed as described (Joyner, 1993). Resistant colonies were picked after 8-10 days of selection. Genomic DNA was extracted from expanded clones, digested with *Hin*dIII and analyzed by Southern blotting at the 3′ end of the recombinant locus. Homologous recombinant clones were analyzed at the 5′ end by *Eco*RI digest and Southern analysis. Out of 1200 ES clones screened, three scored positive for homologous recombination and were propagated.

Generation of chimeric mice and germline transmission of the Ebf2 targeted allele

The targeted ES clones were injected into blastocysts derived from C57BL/6J females. The chimeric embryos were then transferred into the uteri of 2.5 day pseudopregnant foster mothers. Chimeric males with 40-100% agouti color were test-bred by crossing with wild-type C57BL/6J females and germline transmission was identified by the presence of agouti offspring. Heterozygous mice were initially identified by Southern blotting with the 3′ probe. Subsequent genotyping was carried out by PCR amplification with *lacZ*-specific and *Ebf2*-specific primers.

RT-PCR

RNA was extracted by the caesium chloride method from E13 embryos and from postnatal and adult sciatic nerves. Reverse transcription was conducted with oligo-dT and random hexamers, as described previously (Ausubel et al., 1995). A primer pair (F: 5′-TGG AGA ATG ACA AAG AGC AAG; R: 5′-GGG TTT CCC GCT GTT TTC AAA) specific for the cDNA region encoding the Ebf2 DNA-binding domain was used for PCR amplification, according to standard protocols. *Gapdh* primers used for normalization were 5′-CGC ATC TTC TTG TGC AGT G (forward) and 5′-GTT CAG CTC TGG GAT GAC (reverse).

Mouse genetics

The mutation was transferred onto different genetic backgrounds by three distinct procedures: first, we incrossed the transmitting chimeras with 129/SvJ females to transfer the mutation onto a 129/SvJ background and obtain pure coisogenic mutants. Second, we intercrossed (129/SvJ×C57BL/6J)F_1 mice to obtain F_2 homozygotes of heterogeneous genetic backgrounds. Third, we backcrossed (129/SvJ×C57BL/6J)F_1 hybrids with C57BL6/J mice.

Removal of the Neo minigene

The KO construct contains a neomycin minigene (Joyner, 1993). This cassette is flanked by *loxP* sites. In order to exclude a possible effect of the *Neo* minigene on the mutant phenotype, we crossed *Ebf2*$^{+/-}$ mice with transgenic mice expressing the *Cre* recombinase under control of the β-actin promoter. By intercrossing *Cre*+ *Ebf2*$^{+/-}$ transheterozygotes, we obtained *Neo*-negative, *Ebf2*$^{-/-}$ mice, that were *Cre*-negative, formally excluding mosaicism for the *Neo* cassette. Phenotypic and pathological abnormalities observed in those mice were indistinguishable from those scored in *Ebf2*$^{-/-}$, *Neo*-positive mice (data not shown).

lacZ staining procedures

For whole-mount *lacZ* staining, whole tissues were removed from mice anesthetized and transcardially perfused with 0.9% NaCl followed by 4% paraformaldehyde (PFA). Dissected organs were washed in wash buffer (0.01% sodium deoxycolate, 0.02% Nonidet P40, 2 mM magnesium chloride in 1× phoshate buffer) and stained for 2-6 hours at 37°C in staining solution (50 mg X-gal, 0.106 g potassium ferrocyanide and 0.082 g potassium ferricyanide were dissolved in 50 ml of wash buffer).

Histology, immunohistochemistry and immunofluorescence

Embryos and mice were respectively fixed by immersion, or

anesthetized and transcardially perfused with 0.9% NaCl followed by 4% PFA. Brain and testes were postfixed overnight in 4% PFA at 4°C, dehydrated in ethanol, embedded in paraffin wax and cut into 5-7 μm section using a microtome. Sections were counterstained with Cresyl Violet (Sigma) or Hematoxylin And Eosin (Sigma). For immunohistochemistry, tissues were cryoprotected in 30% sucrose, 1×PBS (overnight), included in OCT (Bioptica) and stored at –80°C, before sectioning in a cryotome (5-15 μm). Immunohistochemical analysis was conducted on cryosections with the following antibodies: polyclonal anti GnRH (LR1,1:2000, courtesy of R. Benoit, Montreal), polyclonal anti-peripherin (1:1000, Chemicon) and anti Tag-1 adhesion molecule (courtesy of A. J. W. Furley, Sheffield). Sections were immunostained as suggested (Vector Laboratories), counterstained with Methyl Green (Sigma), dehydrated and mounted with DPX (BDH-Merck).

For dual immunofluorescence, E15 embryo cryosections were treated for 10 minutes with 0.1 M glycine, preincubated in 15% goat serum, 0.2% triton X-100, 1×PBS and incubated overnight at 4°C with the two primary antibodies (polyclonal anti GnRH, 1:1000, monoclonal anti-β-galactosidase, 1:500 Promega). The sections were washed 6 times for 10 minutes in 0.45 M NaCl, 0.3% triton X-100, 20 mM phosphate buffer, rinsed in 1×PBS and incubated for 1 hour at room temperature with the two secondary antibodies (TRITC anti-mouse, 1:150, Jackson ImmunoResearch Laboratories and FITC anti rabbit, 1:150, Sigma). Controls consisted of replacing either the first primary Ab or the second primary Ab with goat serum. Control sections indicated no cross-reactivity between the first and the second Ab.

Electron microscopy

Sciatic nerve specimens were fixed with 2% glutaraldehyde (2-3 hours), postfixed in 1% osmium tetroxide, following ethanol dehydration, and finally embedded in Epon/araldite. Electron microscopy analysis was performed on ultrathin transverse sections made on a Reichert ultramicrotome, stained with uranyl acetate and lead citrate. Slides were examined under a Zeiss electron microscope.

Bromodeoxyuridine labeling and detection

Adult male mice were injected intraperitoneally with 100 mg/kg of bromodeoxyuridine (BrdU, Sigma) and sacrificed 2 hours later. Anti BrdU immunohistochemistry was performed as described (Garel et al., 1997).

Electrophysiological methods

Mice were anesthetized with trichloroethanol, 0.02 ml/g body weight, and placed under a heating lamp in order to avoid hypothermia. Electrophysiological tests were carried out as described (Zielasek et al., 1996). Motor responses were acquired with a Medelec Sapphire 4 Me electromyograph (Medelec, Woking, UK). Statistical analysis was performed by using the Student's *t*-test for unpaired data.

RESULTS

Targeted inactivation of Ebf2

In order to produce a gene targeting construct and inactivate the *Ebf2* gene (Fig. 1), we screened a genomic phage library (129/SvJ) using a probe corresponding to intron 1 of the gene. We isolated two genomic DNA clones spanning 4 kb upstream of the transcription initiation site through exon 6, located 12.5 kb further downstream (Fig. 1A), and generated a targeting construct in which a neomycin resistance minigene (*Pgk-Neo*), preceded by a promoterless *lacZ* cDNA, was used to replace a 5.2 kb stretch encompassing the translation initiation site and the first five exons. This region of the gene encodes the majority of the Ebf2 DNA-binding domain (Malgaretti et al., 1997; Wang et al., 1997). We electroporated embryonic stem (ES) clones with the *Not*I-linearized recombinant plasmid. By standard molecular genetic techniques, we isolated three homologous recombinant ES cell clones that we expanded and used to inject blastocysts. High percentage chimeric males

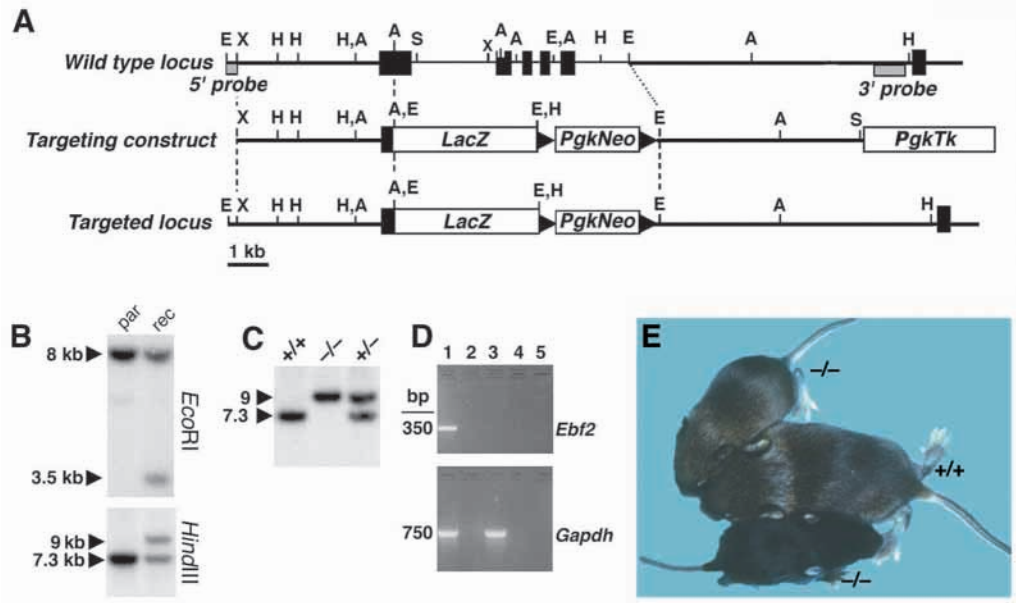

Fig. 1. Generation of *Ebf2*-null mice by homologous recombination. (A) The wild type Ebf2 locus (first six exons only), targeting construct and targeted *Ebf2* locus. Letters represent restriction sites. A, *Apa*I; E, *Eco*RI; H, *Hin*dIII; S, *Sal*I; X, *Xho*I; solid boxes represent exons; stripes represent introns; gray boxes represent genomic sequences used to generate 5′ and 3′ probes; triangles represent loxP sites; the *PgkNeo*, *PgkTk* minigenes and the *lacZ* cDNA are represented as empty boxes. (B) Restriction patterns obtained by hybridizing *Eco*RI-digested DNAs form parental ES cells (par) and homologous recombinant clones (rec) with the 5′ probe, and *Hin*dIII-digested DNAs with the 3′ probe. Fragments corresponding to the recombinant locus are 3.5 kb in *Eco*RI digests and 9 kb in *Hin*dIII digests. (C) Restriction patterns obtained by hybridizing with the 3′ probe *Hin*dIII-digested DNAs from wild type (+/+), heterozygous (+/–) and homozygous mutant (–/–) mice. (D) RT-PCR experiments conducted starting from total RNA from E13 embryos. Lanes 1,2, wild-type RNAs; lanes 3,4, *Ebf2*$^{-/-}$ RNAs; lanes1,3, RT+ experiments; lanes 2,4, RT– controls; lane 5, distilled H_2O was used as template for the PCR reaction (blank). A Gapdh RT-PCR product was used for normalization. The 350 *Ebf2* cDNA fragment failed to amplify from *Ebf2*$^{-/-}$ reverse transcription reactions. (E) General appearance of two 20-day-old F_2 *Ebf2*$^{-/-}$ male mice (–/–) compared with one wild-type F_2 male littermate (+/+).

were mated with C57BL/6J females, and F_1 recombinant progeny were selected based on agouti coat color and genotyping at the *Ebf2* locus. By intercrossing heterozygous mutants [(129/SvJ$^{Ebf2\text{-}lacZ}$×C57BL/6J)F_1] we obtained a percentage of homozygous mutant F_2 mice consistent with expected Mendelian frequencies, suggesting that outbred *Ebf2*$^{-/-}$ mice do not die as embryos.

RT-PCR experiments conducted on total RNA extracted from wild-type and homozygous mutant E13 embryos provided evidence that homozygous mutants produce no *Ebf2* transcript 3′ to the *lacZ* insertion (Fig. 1D). To maximize sensitivity, a similar experiment was conducted on cDNA extracted from the peripheral nerve, with Southern transfer of RT-PCR products followed by hybridization with an *Ebf2* probe, yielding concordant results (not shown).

The *Ebf2* gene is expressed at numerous sites in the nervous system, both before and after birth (Garel et al., 1997; Malgaretti et al., 1997). Taking advantage of the promoterless *lacZ* gene (encoding a cytoplasmic β-galactosidase) integrated into the *Ebf2* locus, we analyzed *Ebf2* expression by histochemical *lacZ* staining. The staining distribution in early development is in full agreement with the results of previous expression studies (Garel et al., 1997; Malgaretti et al., 1997). The present paper will focus on expression sites corresponding to the major morphological changes observed in the mutants.

Phenotype

Fig. 1E shows the phenotypic features of two 20-day-old *Ebf2*$^{-/-}$ males next to a wild-type male littermate. At birth, *Ebf2*$^{-/-}$ mice were hardly distinguishable from *Ebf2*$^{+/-}$ and *Ebf2*$^{+/+}$ ones after gross examination. The first obvious abnormalities became detectable starting at 5 days after birth (P5). *Ebf2*$^{-/-}$ mice were small compared with their *Ebf2*$^{+/+}$ and *Ebf2*$^{+/-}$ littermates: homozygotes weighed less than half the bodyweight of their littermates by P30 (*Ebf2*$^{+/+}$, 16.46±1.84 g, n=9; *Ebf2*$^{+/-}$, 15.34±2.45 g, n=12; *Ebf2*$^{-/-}$, 6.87±1.78 g, n=7; *Ebf2*$^{+/+}$ versus *Ebf2*$^{-/-}$, P<0.0001; *Ebf2*$^{+/-}$ versus *Ebf2*$^{-/-}$, P<0.0001; *Ebf2*$^{+/+}$ versus *Ebf2*$^{+/-}$, not significant). Studies are in progress to define the physiological basis of this growth retardation.

Phenotypic and pathological changes described herein have been scored in mice derived through at least five generations of backcrossing on the C57BL6/J background, in order to minimize the effects of genetic background heterogeneity. Once they reached adulthood, *Ebf2*$^{-/-}$ males and females failed to reproduce when mated to wild-type breeders of the opposite gender. In addition, *Ebf2*$^{-/-}$ mice were mildly uncoordinated and walked with an unsteady, waddling gait. Most noticeably, they exhibited a ‘hunchback’ posture both at rest and, more prominently, while walking.

GnRH-neurons from *Ebf2*-null mice fail to migrate into the hypothalamus

The reproductive failure observed in our mutants suggested several possible explanations, including an alteration in the hypothalamus-pituitary gonadotropic axis, which governs sexual maturation (Wilson et al., 1998). In this respect, we investigated the development of gonadotropin releasing hormone GnRH-neurons; these neurons are initially located in the vomeronasal organ anlage of the nasal placode and subsequently migrate medially and dorsally through the nasal mesenchyme and cribriform plate of the ethmoid bone along the vomeronasal and terminal nerve fibers, then penetrate into the rostral forebrain and move caudally into the septohypothalamic region, where they extend axons towards the median eminence (ME) and infundibulum of the pituitary gland (reviewed by Wray, 2001). In agreement with previous reports (Wang et al., 1997), *lacZ* staining in heterozygous midgestation embryos revealed *Ebf2* expression in the olfactory epithelium, and particularly in the vomeronasal organ (Fig. 2A,B). In *Ebf2*$^{-/-}$ embryos, olfactory and vomeronasal fibers could be detected at all correct locations in the mutant forebrain at embryonic day 15, and stained positive for peripherin (Wray et al., 1994) (Fig. 2D) and for the Tag-1 adhesion molecule (Wolfer et al., 1994) (not shown) in wild-type and mutant mice alike. Furthermore, by histological analysis, we examined olfactory bulb sections obtained from P30 wild-type and null mutant mice. No abnormalities were observed in the cytoarchitecture of this region in *Ebf2*$^{-/-}$ mice (Fig. 2F).

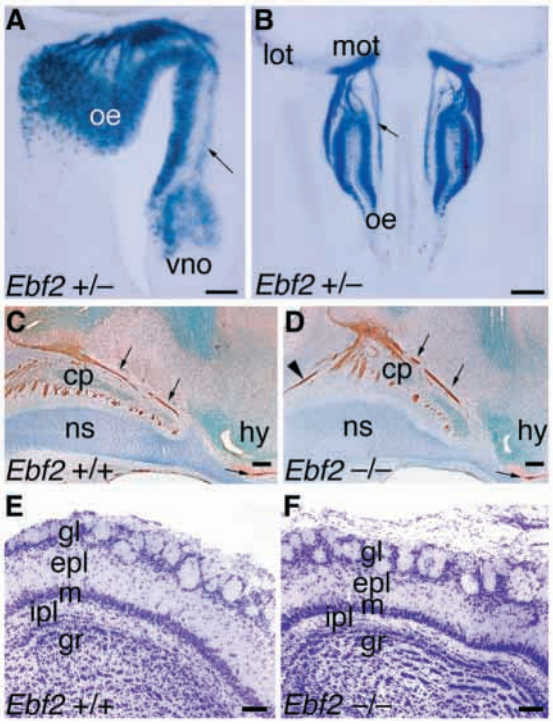

Fig. 2. Olfactory structures develop normally in *Ebf2*-null mice. Histochemical staining conducted on vibratome sections of E12.5 (A) and E13.5 (B)mice. *lacZ* expression can be observed in the olfactory epithelium (oe), in the vomeronasal organ (vno) and alongside olfactory/vomeronasal fibers (arrows). (C,D) Peripherin-positive fibers connecting the olfactory epithelium to the hypothalamus (arrows) are normally distributed in wild-type (C) and mutant (D) embryonic brains alike (arrowhead indicates fibers in the nasal mesenchyme). (E,F) Nissl staining of P30 paraffin coronal sections. The mutant olfactory bulb (F) is histologically indistinguishable from the wild-type one (E). cp, cribriform plate; epl, external plexiform layer; gl, glomerular layer; gr, granule cell layer; hy, hypothalamus; ipl, internal plexiform layer; lot, lateral olfactory tract; m, mitral cell layer; mot, medial olfactory tract; ns, nasal septum; oe, olfactory epithelium; vno, vomeronasal organ. Scale bars: 100 μm in A; 200 μm in B; 150 μm in C,D; 100 μm in E,F.

By dual immunofluorescence, we determined that *Ebf2* is expressed in migrating GnRH-neurons as the onset of their migration, i.e. E11 in the mouse (Schwanzel-Fukuda and Pfaff, 1989) (Fig. 3). Fig. 3 shows colocalization (Fig. 3C) of GnRH (Fig. 3A) and β-galactosidase (B) immunostaining in migrating E15 GnRH-neurons in the null mutant's nasal mesenchyme. We used β-galactosidase-like staining as an unambiguous marker of *Ebf2* expression, as polyclonal anti-Ebf2 antibodies available to us crossreact with other Ebf proteins. At embryonic day 15 (E15), wild-type (wt) GnRH-neurons were mostly located dorsal to the cribriform plate and were navigating caudally towards the preoptic region; conversely, in E15 mutant embryos, most GnRH-neurons were still detected in the nasal mesenchyme (Fig. 4B, Fig. 3A). *Ebf2*$^{-/-}$ neurons were very tightly clustered and in some cases did not show any obvious leading nor trailing processes typical of migrating GnRH-neurons. At birth (P0), GnRH-positive fibers were evident in the ME of the hypothalamus (Fig. 4C), whereas no fibers were detectable in the ME of the mutants (Fig. 4D). Finally, in P30 mutant brains, hardly any GnRH-positive neurons were detected either in the septohypothalamic region (Fig. 4F) or in any region spanning the olfactory bulbs through the anterior commissure. The defect in GnRH-neuron development did not appear to be secondary to abnormal growth or navigation of the olfactory fibers that support their neurophilic migration. In fact these fibers are normally present in null mutants (Fig. 2D).

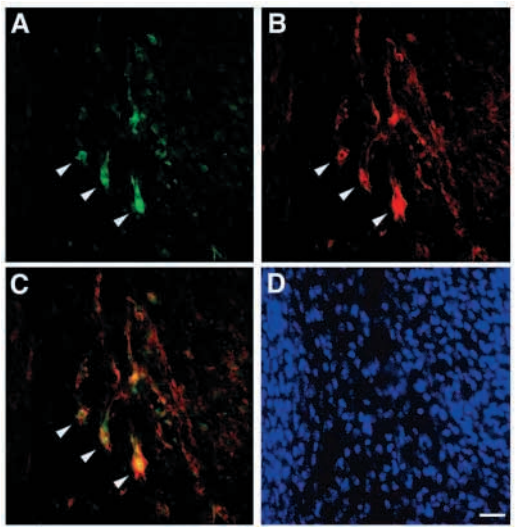

Fig. 3. Migrating GnRH-neurons express Ebf2. Arrowheads in A-C indicate cell bodies of migrating neurons. (A) GnRH-like immunostaining in *Ebf2*$^{-/-}$ neurons migrating dorsally through the nasal mesenchyme at embryonic day 15. (B) Anti β-galactosidase staining in the same neurons. (C) Superimposed signals from A and B revealed co-expression of Ebf2 and GnRH in migrating neurons. (D) Hoechst nuclear counterstaining of same field. As described (Wray, 2001), GnRH-neurons migrate through cell-poor, nerve fiber-rich regions. Scale bar: 20 μm.

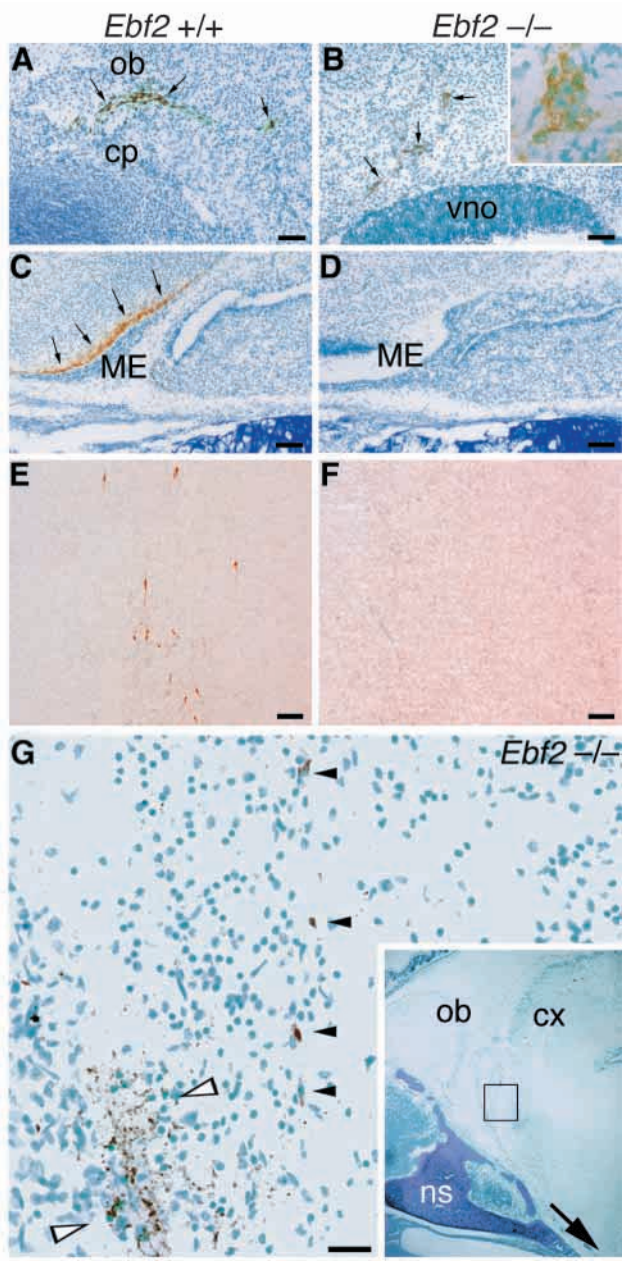

Fig. 4. Defective migration of GnRH-neurons from the olfactory epithelium to the hypothalamus. (A,C,E) Normal controls; (B,D,F,G) *Ebf2*$^{-/-}$ coisogenic mutants; (A,B) E15; (C,D,G) P0; (E,F) P30. (A) In E15 wild-type embryos, migrating GnRH-neurons (arrows, brown staining, nuclear counterstaining in cyan) are mostly located dorsal to the cribriform plate (cp) and ventral to the olfactory bulb (ob). (B) Mutant neurons (arrows) migrate slowly out of the vomeronasal organ (vno). (Inset) Mutant neurons form dense clusters, often devoid of leading or trailing processes. (C) GnRH-positive fibers (arrows) reach the median eminence (ME) of the hypothalamus in wild-type newborn brains. (D) No GnRH immunostaining in the ME of mutant P0 brains. (E) GnRH-positive neurons (brown) in the preoptic region of the wild-type hypothalamus. (F) No GnRH immunostaining in the corresponding region of mutant brains. (G) At birth, mutant GnRH-positive neuronal cell bodies (black arrowheads) and fibers (white arrowheads) are ectopically located in the forebrain close to the midline at the interface between olfactory bulb (ob) and rostral telencephalic cortex (cx), dorsal to the nasal septum (ns) and cribriform plate. See empty box in inset for localization. Arrow in inset indicates physiological migration route. cp, cribriform plate; cx, telencephalic cortex; ME, median eminence; ns, nasal septum; ob, olfactory bulb; vno, vomeronasal organ. Scale bars: 100 μm in A-F; 50 μm in G.

Based on the above observations, we investigated the eventual fate of GnRH-neurons in *Ebf2*$^{-/-}$ mice. As mentioned earlier, at E15 most neurons were abnormally retained in the nasal cavity of *Ebf2*$^{-/-}$ embryos, unlike in their wild-type counterparts. Hoechst counterstaining of these neurons revealed that in most cases their nuclei had indented borders and fuzzy to undiscernible nucleoli, suggesting that neurons that failed to migrate eventually degenerated (not shown). Neuronal degeneration appeared to be secondary to defective migration, as numerous neurons were still found in the nasal mesenchyme 5.5 days after their birth in the vomeronasal organ. Although migration of most GnRH-neurons was arrested in the nasal mesenchyme or just dorsal to the cribriform plate, a subset of GnRH-immunoreactive neurons were found in the forebrain at birth, at the caudal boundary of the olfactory bulb (Fig. 4G).

Consistent with the observed defect in GnRH-neuron development, inbred *Ebf2*$^{-/-}$ mice were hypogonadic and failed to reproduce or to exhibit any mating behavior when caged with wild-type C57BL6/J breeders. This statement refers to a cumulative period of over 14 months of random matings (n=3 homozygous mutant males; n=3 homozygous mutant females). At birth, homozygous mutants displayed completely formed testes, that were similar in size to their littermates. Conversely, inspection of post-pubertal (P45, P60) male gonads showed a dramatic disparity in their volume in *Ebf2*$^{-/-}$ and *Ebf2*$^{+/+}$ males (*Ebf2*$^{+/+}$: 3.29±0.14 mm, n=4; *Ebf2*$^{-/-}$: 2.22±0.05 mm, n=4; P=0.0004). Histological examination of *Ebf2*$^{-/-}$ male gonads indicated testis hypoplasia without Leydig cell hyperplasia. This was consistent with hypogonadotropic hypogonadism and argued strongly against an intrinsic defect of the seminipherous tubule. Testes displayed a reduction of the interstitial component, similar to what has been observed in hypogonadal (hpg) mice (Cattanach et al., 1977), which carry an intragenic deletion in the *Gnrh*-gene (Mason et al., 1986). While Sertoli cells from normal and *Ebf2*$^{-/-}$ mice were morphologically indistinguishable, mutant seminipherous tubules contained fewer dividing spermatogonia (Fig. 5D) compared with wild-type tubules, as assayed by BrdU incorporation. Likewise, mutant epidydimes had a reduced diameter and contained very few sperm cells (Fig. 5F), when compared with control wild-type epidydimes.

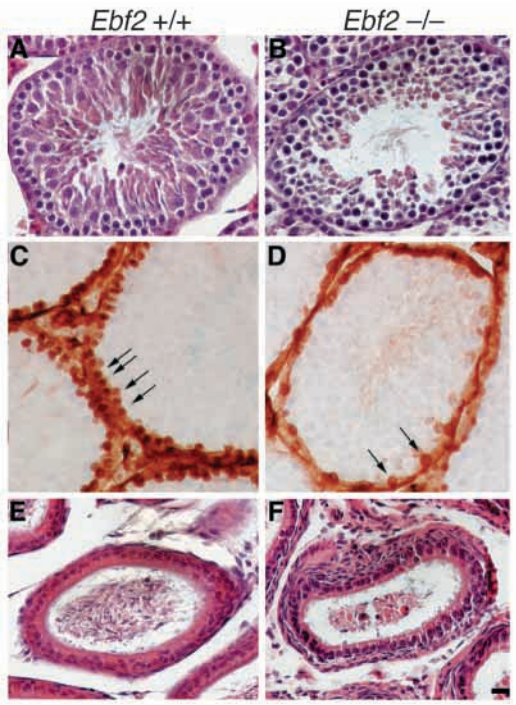

Fig. 5. Hypoplasia of seminipherous tubules and reduced spermatogenesis in *Ebf2*-null mice. (A,C,E) Wild type; (B,D,F) *Ebf2*$^{-/-}$. (A,B) Hematoxylin and Eosin (HE) staining of seminipherous tubules. In B, the luminal side of the tubule contains very few aggregations of spermatids compared with wild-type tubule. (C,D) Anti BrdU immunostaining reveals a sharply reduced number of proliferating spermatogonia in mutant tubules (arrows). (E,F) HE-stained epidydimes. The lumen of a mutant epidydimis (F) contains cell debris and hardly any sperm cells. The latter are recognizable as Hematoxylin-stained (dark purple) dots in the normal control (E). Scale bar: 40 μm.

Morphological and functional defects in the mutant peripheral nervous system

The defects observed in the development of GnRH-synthesizing neurons were not the only morphogenetic abnormalities observed in the CNS of *Ebf2*$^{-/-}$ mice. In fact, null mutants exhibited substantial defects in cerebellar morphogenesis that are beyond the scope of the present study, and are being actively investigated by our group (L. C. and S. Z., unpublished). In addition, major defects were also observed in the *Ebf2*$^{-/-}$ peripheral nervous system.

In a systematic analysis of *Ebf2* gene expression, we found *Ebf2* expression in the embryonic and postnatal spinal cord, dorsal root ganglia and peripheral nerve (Fig. 6). A detailed analysis of *lacZ* expression in the mutant mice provided us with new information in addition to that stemming from previous studies. At E12.5, *Ebf2* was expressed in dorsal root ganglia (DRG), as reported previously (Garel et al., 1997; Malgaretti et al., 1997). However, its expression (blue signal in Fig. 6A) was clearly confined to presumptive satellite cells negative for the heavy chain neurofilament (NF-H). Likewise, dorsal root fibers positive for NF-H were negative for cytoplasmic *lacZ*, while presumptive peripheral glial progenitors intercalated to those fibers were positive (blue signal in Fig. 6B). In agreement with this, E16.5 immature glial progenitors positive for the low-affinity nerve growth factor receptor p75 were also positive for *lacZ* staining (Fig. 6C). In P15 sciatic nerves from null mice, *Ebf2* was expressed in both myelin forming (msc) (arrows in Fig. 6D,E) and non-myelin forming Schwann cells (nmsc) (arrowhead in Fig. 6D), while in heterozygous mice *Ebf2* expression was detected only in nmsc (arrows in Fig. 6F). In the P30 spinal cord, *Ebf2* was expressed in dorsal interneurons (lamina 2), in the commissural gray matter and in other as yet undefined neural cells localized in dorsal, and commissural areas of the spinal cord (blue signal in Fig. 6G). Finally, in Fig. 6H a high magnification of ventral region of the spinal cord revealed colocalization of *Ebf2* (in blue) with choline acetyltransferase, a motoneuron marker (brown). Unlike in postnatal development, *Ebf2* was not obviously expressed in islet 1-positive motoneuron precursors at E10 (Garel et al., 1997) or at subsequent midgestation embryonic stages (L. C. and G. G. C., unpublished).

In keeping with the evidence of *Ebf2* expression throughout glial cell differentiation and in postnatal motoneurons, *Ebf2*-

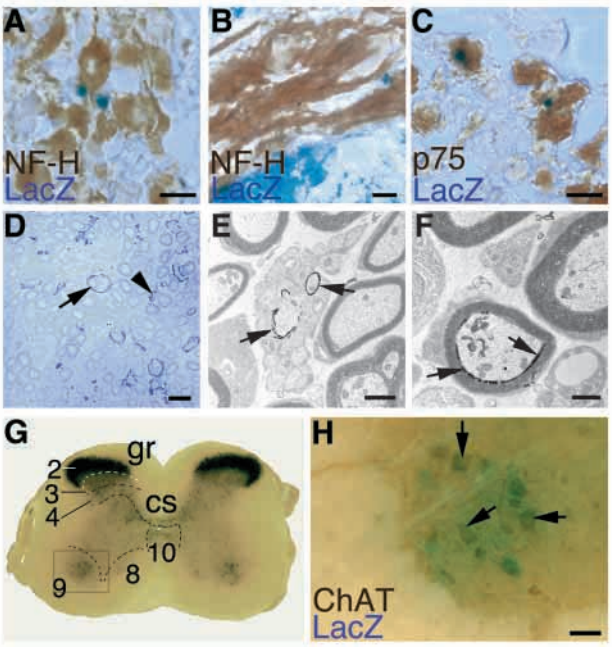

Fig. 6. Ebf2 is expressed in embryonic, postnatal glia and in postnatal motoneurons. (A) E12.5 DRG neurons positive for the heavy chain neurofilament (NF-H) are negative for *lacZ* staining (Ebf2); however, *lacZ* staining is observed in presumptive satellite cells adjacent to NF-H positive neurons. (B) In E12.5 dorsal roots, NF-H-like staining corresponding to DRG neuron axons does not colocalize with *lacZ* staining. (C) In E16.5, peripheral glial cell precursors are positive for p75 NGFR and *lacZ*. (D) In semi-thin transverse sections of P15 null mutant sciatic nerve, Ebf2 (*lacZ* staining) is expressed in both myelin forming (msc, arrow) and non-myelin forming (nmsc, arrowhead) Schwann cells. (E) Electron microscopy (EM) image of a heterozygous P15 sciatic nerve stained with bluo-gal, revealing Ebf2 expression (arrows) in nmsc. (F) EM image of a P15-null mutant nerve stained with bluo-gal, revealing persistent expression of Ebf2 in mutant msc (arrows). (G) Low-magnification image of a vibratome transverse section of an heterozygous P30 spinal cord, at the level of the lumbar swelling, revealing Ebf2 expression in dorsal (2,3), commissural (4,10) and ventral (9) laminae of the gray matter. H corresponds to the boxed area in G and reveals Ebf2 colocalization (arrows) with the motoneuron marker choline acetyltransferase (ChAT). 2-9, spinal cord layers 2-9; cs, corticospinal tract; gr, fasciculus gracilis. Scale bars: 10 μm in A,C; 5 μm in B; 10 μm in D; 2 μm in E; 1 μm in F; 80 μm in H.

null sciatic nerves showed various abnormalities in their postnatal development. At gross examination, sciatic nerve trunks came apart spontaneously during surgical manipulation. Histological analysis of Toluidine Blue-stained semi-thin sections revealed that axons, especially large caliber ones, were considerably hypomyelinated in the *Ebf2*$^{-/-}$ sciatic nerve (Fig. 7). Likewise, ultrastructural analysis of *Ebf2*$^{-/-}$ nerves revealed several abnormalities. As previously described (Webster et al., 1973), by P15 wild-type sciatic nerves display a complete segregation of large axons (≥1 μm across) from smaller ones. The former establish a one-to-one relationship with MSC and become myelinated; the latter are fasciculated together by each NMSC and wrapped by cytoplasmic lamellae, remaining unmyelinated (Fig. 8A). Conversely, examination of mutant nerves revealed many unsorted medium to large axons (1-4

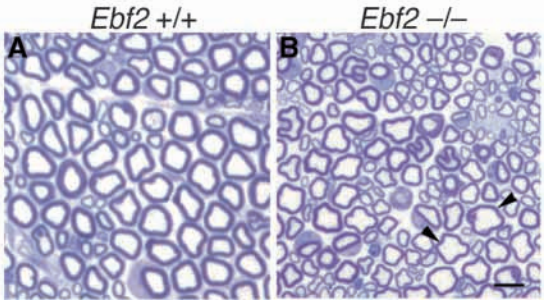

Fig. 7. Large axons are hypomyelinated in the *Ebf2*$^{-/-}$ sciatic nerve. (A) Toluidine Blue-stained transverse semi-thin section of a wild-type sciatic nerve at postnatal day 30. (B) Section of a P30 *Ebf2*-null sciatic nerve that corresponds to that in A. Note reduced myelin thickness of sample large caliber *Ebf2*$^{-/-}$ axons indicated by arrowheads in B, in comparison with *Ebf2*$^{+/+}$ fibers of similar sizes in A. Scale bar: 10 μm.

μm) that failed to be myelinated. Even in adult nerves (P30), these were fasciculated into anomalous bundles next to smaller axons (Fig. 8B). Occasionally, unsorted axons still wrapped by NMSC cytoplasm became abnormally myelinated (Fig. 8C). Longitudinal sections clearly demonstrated that in some cases myelinated and unmyelinated segments belonged to consecutive internodes of the same axon, constituting a case of segmental dysmyelination (Fig. 8D). In addition, some myelinated fibers featured abnormally thin myelin sheaths (Fig. 8E). With nerve maturation, signs of axonopathy became apparent: starting at about P15, it became possible to observe features of axonal damage, such as accumulations of vesicular, membrane-bound material in the axon (Fig. 8F).

Based on the morphological abnormalities observed in mutant nerves, we conducted electrophysiological tests on adult, age- and gender-matched homozygous mutants (n=9) and controls (n=8). We stimulated the sciatic nerve at the ankle and at the ischiatic notch; the compound motor action potential (cMAP) was recorded from the paw muscles with a pair of needle electrodes to measure motor nerve conduction velocity (NCV). The mean values of NCV, compound motor axon potential (cMAP) latencies and amplitude, and F-wave latencies are summarized in Table 1. The main finding emerging from our studies was a striking reduction (by 40%) of NCV in the knockout group when compared with the wild-type group. All members of the knockout group scored lower in terms of NCV than controls. The mean amplitude of motor responses was also significantly decreased in comparison with controls, although cMAP amplitude data should be interpreted cautiously when dealing with needle recordings. Likewise, although the mean value of F-wave latency was found to be significantly higher in mutant nerves, this finding may simply reflect the overall decrease in NCV. Actually, the finding of measurable F-wave recordings in the mutant group ruled out a conduction block at the level of proximal nerve segments or spinal roots.

DISCUSSION

Both gain-of-function (Dubois et al., 1998; Pozzoli et al., 2001) and loss-of-function (Garel et al., 1999; Prasad et al.,

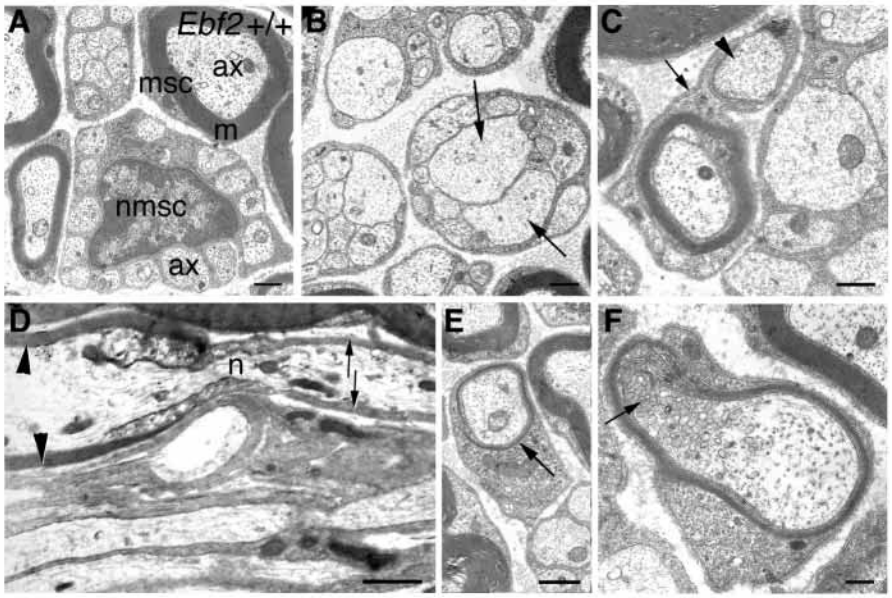

Fig. 8. Defective axon sorting, dysmyelination and axonal degeneration in the mutant sciatic nerve. (A) Normal control nerve at postnatal day 30 (P30); note orderly arrangement of uniformly sized axons sorted within the cytoplasm of a non-myelin forming Schwann cell (nmsc), and, in parallel, a myelin forming Schwann cell (msc) surrounding a single large diameter axon (ax) with a myelin cuff (m). (B-F) sciatic nerve sections from *Ebf2*$^{-/-}$ mice. (B) At P30, two 4 μm axons (arrows) are abnormally fasciculated within the cytoplasm of a nmsc. Likewise, in C (P60), a single Schwann cell ensheathes an unmyelinated axon and a myelinated one; arrow indicates SC basal lamina joining myelinated and unmyelinated axons; note adjacent unmyelinated 3 μm axon (arrowhead). (D) A longitudinal section from a P45 nerve reveals segmental dysmyelination: an internode is myelinated (arrowheads) proximal to a node (n), while the subsequent internode remains unmyelinated (arrows). (E) A hypomyelinated axon at P60, a stage at which myelination is complete in controls; arrow indicates an abnormally thin myelin sheath. (F) A P30 axon shows cytoplasmic vacuoles (arrow), indicative of axonal degeneration. ax, axon; m, myelin; msc, myelin-forming Schwann cell; n, node of Ranvier; nmsc, nonmyelin-forming Schwann cell. Scale bars: 1 μm in A-E; 0.5 μm in F.

1998) evidence obtained in various model organisms implicates Ebf genes in key stages of neural development. Although the three known Ebf genes are widely co-expressed in the developing neural tube (Garel et al., 1997), recent evidence has led to the proposal of distinct developmental roles for vertebrate Ebf family members, and specifically differential control of their expression and transactivating functions (Pozzoli et al., 2001).

Our data are consistent with the notion that proteins belonging to the Ebf network play some redundant roles. Overall, *Ebf2*$^{-/-}$ mice complete embryonic development successfully, albeit displaying subtle abnormalities that are beyond the scope of the present study. However, our evidence also indicates that some specific morphogenetic processes clearly require *Ebf2*, despite the fact that other Ebf genes are co-expressed with it. For example, although *Ebf1* is co-expressed with *Ebf2* in migrating GnRH-neurons (Wray, 2001), their migration is defective in *Ebf2* mutants. Likewise, although both *Ebf1* and *Ebf3* are co-expressed with *Ebf2* in the postnatal nerve (L. C. and G. G. C., unpublished), nerve organization and conduction are clearly altered in *Ebf2*$^{-/-}$ mice.

Table 1. Analysis of nerve conduction in adult *Ebf2*$^{-/-}$ mice

	Mean±s.d.		
	Wild type (*n*=8)	*Ebf2*$^{-/-}$ (*n*=9)	*P* value
Conduction velocity (m/second)	35.28±2.68	21.81±2.97	<0.0001
Proximal amplitude (mV)	7.39±2.57	5.00±2.62	Not significant
Distal amplitude (mV)	9.35±2.64	6.29±2.73	0.03
Distal latency (mseconds)	1.11±0.13	1.07±0.09	Not significant
F wave (mseconds)	4.95±0.40	6.10±0.92	0.005

Statistical analysis was performed using Student's *t*-test for unpaired data. Threshold for significance: $P \leq 0.05$.

The study of *Ebf2*$^{-/-}$ embryos indicates that *Ebf2* is not required for the birth of GnRH-neurons, or that redundant mechanisms are in place to offset the lack of *Ebf2* in this function. However, our mutants show a clear impairment in GnRH-neuron migration from the olfactory epithelium to the diencephalon. In particular, GnRH-neurons exit the nasal mesenchyme later than in wild-type mice, and show signs of degeneration. Those mutant neurons that manage to reach dorsal to the cribriform plate, fail to deflect caudally into the ventral forebrain. Instead, they move dorsally through the rostral telencephalon, possibly along the dorsal branch of the vomeronasal nerve. Altered migration of GnRH-neurons has been observed in other animal models. For example, it has been reported that enzymatic removal of polysialic acid from NCAM-rich vomeronasal nerves at E12 significantly inhibits the migration of GnRH-neurons, without affecting the vomeronasal tract itself (Yoshida et al., 1999). The same authors found that NCAM180 knockout mutants show a shift in the migratory route of GnRH cells, resulting in an excess number of these neurons in the accessory olfactory bulb. Likewise, *Dcc* (deleted in colorectal cancer, which encodes a netrin-1 receptor) knockout mice revealed GnRH neurons that were misrouted into the cerebral cortex (Schwarting et al., 2001). However, these mutants could not be studied at later stages, because of postnatal lethality. In both genetic mutants cited above, the impairment of GnRH-neuron migration is accompanied by malformation of the vomeronasal nerve. Conversely, no alterations have been observed in *Ebf2*$^{-/-}$ vomeronasal nerve axons, either by histology or using specific surface markers (Wolfer et al., 1994; Wray et al., 1994). Likewise, no changes have been found in the olfactory bulbs of null mutants (Fig. 2F). In other mutants (Yoshida et al.,

1999), a significant number of GnRH-neurons appear to follow a normal migratory route into the diencephalon and to send projections to the ME, in keeping with the existence of different GnRH-neuron subpopulations or heterogeneity of the migratory pathway (Skynner et al., 1999; Tobet et al., 1996; Wray et al., 1994). In *Ebf2*$^{-/-}$ mice we observed a virtually complete lack of immunoreactive fibers in the ME, and a complete lack of immunoreactivity throughout the septohypothalamic region; this evidence, along with the observed expression of *Ebf2* in GnRH neurons, strongly supports a fundamental role for the Ebf2 protein in GnRH-neuron development. Previous studies have shown that mutation of another Ebf family member (*Ebf1*) (Lin and Grosschedl, 1995) results in a subpopulation of facial branchiomotor neurons adopting a rhombomere 6-specific short-range migration pattern in rhombomere 5, in the embryonic hindbrain (Garel et al., 2000). Not only are our findings consistent with those observations, but they clearly implicate *Ebf2* as a primary factor in the long range developmental migration of an entire population of neuroendocrine neurons. As the *Ebf2* gene is expressed both in GnRH and vomeronasal neurons, our results allow no conclusions to be drawn as to whether the observed migration defect is cell-autonomous, or secondary to the lack of axonal cues. Transgenic approaches should make it possible to solve this riddle, shedding further light on the role of *Ebf2* in neuronal migration.

To the authors' knowledge this is the first report of a single genetic defect that directly affects GnRH-neuron migration with no gross alterations of their migration substrate. In this respect, our findings differ substantially from those reported in a fetus with Kallmann Syndrome (KS), where the defect in GnRH-neuron migration is accompanied by atrophy of the olfactory bulb (Schwanzel-Fukuda et al., 1989). Several genes have been proposed as potential candidates for other forms of KS or for idiopathic hypogonadotropic hypogonadism (HH). These include GnRH receptors, the *LH* and *FSH* genes, and *DAX1*, etc. (Layman, 1999). The evidence reported in the present paper indicates the human ortholog of *Ebf2* as a solid functional candidate for genetic studies of HH. Curiously, by computer analysis of the human genome sequence, we determined that the *EBF2* gene maps within 450 kb of the *GNRH* in human chromosomal band 8p21.

In agreement with the observed CNS defects, examination of post-pubertal mutant mice shows clear evidence of testis hypoplasia in the absence of Leydig cell hyperplasia. The presence of testes, albeit hypoplastic, in these animals excludes an essential role for *Ebf2* in the prenatal stages of gonadal development, and is coherent with the observation that, during fetal development, differentiation and proliferation of both Sertoli and Leydig cells are independent of endogenous gonadotropins (Baker and O'Shaughnessy, 2001; Griswold, 1993; Lejeune et al., 1998). Not surprisingly, testicular abnormalities seen in *Ebf2*$^{-/-}$ mice are superimposable with those observed in hypogonadal (hpg) mice, which carry a null mutation of the *Gnrh* gene, and, therefore, fail to produce gonadotropins (Mason et al., 1986).

The second most striking abnormality in *Ebf2*$^{-/-}$ mutants resides in the peripheral nerve. *Ebf2* is expressed in peripheral glial cell progenitors starting at E12.5, and remains expressed throughout birth in immature Schwann cells, and through adulthood in nmsc. The defect in the developmental downregulation of *Ebf2* transcription observed in msc from null mutant mice suggests an important role for this gene in late embryonic and postnatal development of those cells. In addition to Schwann cells, *Ebf2* is also expressed in postnatal motoneurons. The sciatic nerve of *Ebf2* mutants features glial and axonal defects. These include incomplete axon sorting, which results in defective axonal fasciculation. The notion of an evolutionarily conserved role for Ebf family members in axon fasciculation is supported by the abnormal organization observed in the ventral nerve cord of *unc-3* mutant nematodes, that carry a mutation within an Ebf homolog (Prasad et al., 1998).

In parallel to a clear defect in axonal sorting, *Ebf2*$^{-/-}$ nerves feature signs of segmental dysmyelination and hypomyelination. In fact, the finding of large unsorted axons in transverse nerve sections and that of segmentally unmyelinated axons in longitudinal sections may be linked features of a common defect, whereby large axons fail to establish contacts with msc throughout their length, and as a consequence, are myelinated discontinuously. However, persistent expression of the *lacZ* reporter gene in *Ebf2*$^{-/-}$ msc may also suggest a direct role for *Ebf2* in msc terminal differentiation (which may, in turn, explain the finding of hypomyelinated axons in the adult nerve).

Consistent with the observed signs of dysmyelination, electrophysiological tests reveal a 40% decrease in NCV in mutant nerves, suggesting that currents may leak across the unmyelinated membrane, hampering an efficient action potential propagation. Again, in keeping with the segmental nature of the defect, our conduction studies do not disclose any electrophysiological hallmarks of widespread demyelination, such as a temporal dispersion and polyphasia of motor responses, or a significant proximal-to-distal amplitude decrement. Although segmental dysmyelination is expected to slow down conduction, altered expression or defective clustering of Na^+ or K^+ channels in the nodal and juxtaparanodal regions, respectively, may offer an alternative or additional explanation. Further studies are required to address this point.

In conclusion, through a genetic approach, we have implicated the *Ebf2* gene in the pathogenesis of two phenotypic defects of potential relevance in medical genetics, namely hypogonadotropic hypogonadism and peripheral neuropathy with segmental dysmyelination. In addition, our data provide evidence for a pivotal role of *Ebf2* in the formation of the neuroendocrine axis, which supports pubertal development, and in several morphogenetic events required for peripheral nerve maturation. Molecular and biochemical studies are now required to dissect the genetic circuits involved in those processes.

We thank F. Zanoni, and C. Mocchetti for their important contribution to this project; A. Ballabio for granting us access to the microinjection facility at the Telethon Institute of Genetics and Medicine; and Giulio Cossu and Monica Vetter for critical reading of the manuscript. The financial support of grants 1216 and E.501 by the Italian Telethon Foundation to G. G. C. was essential for our work and is most gratefully acknowledged. R. M. is funded by Telethon grant E.523. A. C. was the recipient of an EMBO short-term fellowship.

REFERENCES

Ausubel, F. M., Brent, R., Kingstone, R. E., Moore, D. D., Smith, J. A. and Struhl, K. (1995). *Current Protocols in Molecular Biology*. New York: J. Wiley and Sons.

Baker, P. J. and O'Shaughnessy, P. J. (2001). Role of gonadotrophins in regulating numbers of Leydig and Sertoli cells during fetal and postnatal development in mice. *Reproduction* **122**, 227-234.

Cattanach, B. M., Iddon, C. A., Charlton, H. M., Chiappa, S. A. and Fink, G. (1977). Gonadotrophin-releasing hormone deficiency in a mutant mouse with hypogonadism. *Nature* **269**, 338-340.

Crozatier, M. and Vincent, A. (1999). Requirement for the Drosophila COE transcription factor Collier in formation of an embryonic muscle: transcriptional response to notch signalling. *Development* **126**, 1495-1504.

Dubois, L., Bally-Cuif, L., Crozatier, M., Moreau, J., Paquereau, L. and Vincent, L. (1998). XCoe2, a transcription factor of the Col/Olf-1/EBF family involved in the specification of primary neurons in *Xenopus*. *Curr. Biol.* **8**, 199-209.

Dubois, L. and Vincent, A. (2001). The COE–Collier/Olf1/EBF–transcription factors: structural conservation and diversity of developmental functions. *Mech. Dev.* **108**, 3-12.

Garel, S., Marin, F., Mattei, M. G., Vesque, C., Vincent, A. and Charnay, P. (1997). Family of Ebf/Olf-1-related genes potentially involved in neuronal differentiation and regional specification in the central nervous system. *Dev. Dyn.* **210**, 191-205.

Garel, S., Marin, F., Grosscheld, R. and Charnay, P. (1999). Ebf1 controls early cell differentiation in the embryonic striatum. *Development* **126**, 5285-5294.

Garel, S., Garcia-Dominiguez, M. and Charnay, P. (2000). Control of the migratory pathway of facial branchiomotor neurones. *Development* **127**, 5297-5307.

Griswold, M. (1993). Action of FSH on mammalian Sertoli cells. In *The Sertoli Cell* (ed. L. D. Russel and M. D. Griswold), pp. 493-508. Clearwater: Cache River Press.

Hagman, J., Belanger, C., Travis, A., Turck, C. and Grosschedl, R. (1993). Cloning and functional characterization of early B-cell factor, a regulator of lymphocyte-specific gene expression. *Genes Dev.* **7**, 760-773.

Joyner, A. L. (1993). *Gene Targeting – A Practical Approach*. Oxford: IRL Press.

Kudrycki, K., Stein-Izsak, C., Behn, C., Grillo, M., Akeson, R., Margolis, F. L., Wang, M. M., Tsai, R. Y., Schrader, K. A. and Reed, R. R. (1993). Olf-1-binding site: characterization of an olfactory neuron-specific promoter motif. *Mol. Cell. Biol.* **13**, 3002-3014.

Layman, L. C. (1999). The molecular basis of human hypogonadotropic hypogonadism. *Mol. Genet. Metab.* **68**, 191-199.

Lejeune, H., Habert, R. and Saez, J. M. (1998). Origin, proliferation and differentiation of Leydig cells. *J. Mol. Endocrinol.* **20**, 1-25.

Lin, H. and Grosschedl, R. (1995). Failure of B-cell differentiation in mice lacking the transcription factor EBF. *Nature* **376**, 263-267.

Malgaretti, N., Pozzoli, O., Bosetti, A., Corradi, A., Ciarmatori, S., Panigada, M., Bianchi, M., Martinez, S. and Consalez, G. G. (1997). *Mmot1*, a new helix-loop-helix transcription factor gene displaying a sharp antero-posterior expression boundary in the embryonic mouse brain. *J. Biol. Chem* **272**, 17632-17639.

Mason, A. J., Hayflick, J. S., Zoeller, R. T., Young, W. S., 3rd, Phillips, H. S., Nikolics, K. and Seeburg, P. H. (1986). A deletion truncating the gonadotropin-releasing hormone gene is responsible for hypogonadism in the hpg mouse. *Science* **234**, 1366-1371.

Pozzoli, O., Bosetti, A., Croci, L., Consalez, G. G. and Vetter, M. L. (2001). Xebf3 is a regulator of neuronal differentiation during primary neurogenesis in Xenopus. *Dev. Biol.* **233**, 495-512.

Prasad, B. C., Ye, B., Zackhary, R., Schrader, K., Seydoux, G. and Reed, R. R. (1998). unc-3, a gene required for axonal guidance in Caenorhabditis elegans, encodes a member of the O/E family of transcription factors. *Development* **125**, 1561-1568.

Schwanzel-Fukuda, M. and Pfaff, D. W. (1989). Origin of luteinizing hormone-releasing hormone neurons. *Nature* **338**, 161-164.

Schwanzel-Fukuda, M., Bick, D. and Pfaff, D. W. (1989). Luteinizing hormone-releasing hormone (LHRH)-expressing cells do not migrate normally in an inherited hypogonadal (Kallmann) syndrome. *Mol. Brain Res.* **6**, 311-326.

Schwarting, G. A., Kostek, C., Bless, E. P., Ahmad, N. and Tobet, S. A. (2001). Deleted in colorectal cancer (DCC) regulates the migration of luteinizing hormone-releasing hormone neurons to the basal forebrain. *J. Neurosci.* **21**, 911-919.

Skynner, M. J., Slater, R., Sim, J. A., Allen, N. D. and Herbison, A. E. (1999). Promoter transgenics reveal multiple gonadotropin-releasing hormone-I- expressing cell populations of different embryological origin in mouse brain. *J. Neurosci.* **19**, 5955-5966.

Tobet, S. A., Chickering, T. W., King, J. C., Stopa, E. G., Kim, K., Kuo-Leblank, V. and Schwarting, G. A. (1996). Expression of gamma-aminobutyric acid and gonadotropin-releasing hormone during neuronal migration through the olfactory system. *Endocrinology* **137**, 5415-5420.

Vervoort, M., Crozatier, M., Valle, D. and Vincent, A. (1999). The COE transcription factor Collier is a mediator of short-range Hedgehog-induced patterning of the Drosophila wing. *Curr. Biol.* **9**, 632-639.

Wang, M. M. and Reed, R. R. (1993). Molecular cloning of the olfactory neuronal transcription factor Olf-1 by genetic selection in yeast. *Nature* **364**, 121-126.

Wang, S. S., Tsai, R. Y. L. and Reed, R. R. (1997). The characterization of the Olf-1/EBF-like HLH transcription factor family: implications in olfactory gene regulation and neuronal development. *J. Neurosci.* **17**, 4149-4158.

Wang, S. S., Betz, A. G. and Reed, R. R. (2002). Cloning of a novel Olf-1/EBF-like gene, O/E-4, by degenerate oligo-based direct selection. *Mol. Cell. Neurosci.* **20**, 404-414.

Webster, H. d., Martin, J. R. and O'Connell, M. F. (1973). The relationships between interphase Schwann cells and axons before myelination: a quantitative electron microscopic study. *Dev. Biol.* **32**, 401-416.

Wilson, J., Foster, D., Kronenberg, H. and Larsen, P. (1998). *Williams' Textbook of Endocrinology*. London: WB Saunders Company.

Wolfer, D. P., Henehan-Beatty, A., Stoeckli, E. T., Sonderegger, P. and Lipp, H. P. (1994). Distribution of TAG-1/axonin-1 in fibre tracts and migratory streams of the developing mouse nervous system. *J. Comp. Neurol.* **345**, 1-32.

Wray, S. (2001). Development of luteinizing hormone releasing hormone neurones. *J. Neuroendocrinol.* **13**, 3-11.

Wray, S., Key, S., Qualls, R. and Fueshko, S. M. (1994). A subset of peripherin positive olfactory axons delineates the luteinizing hormone releasing hormone neuronal migratory pathway in developing mouse. *Dev. Biol.* **166**, 349-354.

Yoshida, K., Rutishauser, U., Crandall, J. E. and Schwarting, G. A. (1999). Polysialic acid facilitates migration of luteinizing hormone-releasing hormone neurons on vomeronasal axons. *J. Neurosci.* **19**, 794-801.

Zielasek, J., Martini, R. and Toyka, K. V. (1996). Functional abnormalities in P0-deficient mice resemble human hereditary neuropathies linked to P0 gene mutations. *Muscle Nerve* **19**, 946-952.